HETEROCYCLES, Vol. 106, No. 12, 2023, pp. -. © 2023 The Japan Institute of Heterocyclic Chemistry
Received, 31st October, 2023, Accepted, 24th November, 2023, Published online, 29th November, 2023
DOI: 10.3987/COM-23-14922

EVALUATION OF 4,4'-DIAMINODIPHENYLMETHANE AS A PLATFORM FOR PROTON, pH, AND METAL ION RESPONSIVE FLUORESCENT PROBE

Takaaki Miyazaki,* Shunsaku Watanabe, Shoko Oka, Taiyou Tsutsumi, and Osamu Hayashida*

Department of Chemistry, Faculty of Science, Fukuoka University, 8-19-1 Nanakuma, Jonan-ku, Fukuoka 814-0180, Japan; email: t.miyazaki@fukuoka-u.ac.jp

Abstract – 4,4'-Diaminodiphenylmethane (DPM)-based fluorescent probes have been reported. We designed a new fluorescent probe **1**, having bis(4-methoxyphenyl)maleimide and an amino group as a fluorophore and a sensing part, respectively, in which DPM was used as a platform for sensing molecules to utilize its advantage. The fluorescence intensity of **1** increased upon adding trifluoroacetic acid in MeCN, CH_2Cl_2, and toluene, indicating that **1** showed as a proton sensor. The fluorescence spectral change of **1** was observed in a mixture of MeCN and various pH buffers. Moreover, **1** behaved as a metal (zinc or nickel) ion sensor with 2-formylpyridine by forming the Schiff base skeleton. The metal ion sensing behavior of **1** could be applied to an AND circuit.

INTRODUCTION

4,4'-Diaminodiphenylmethane (DPM), composed of two aniline units linked with an sp^3-carbon atom, has been used as a fundamental component for polymers[1–4] and coordination cages,[5] due to its easy modification of the amino groups. Our group has also studied DPM-based water-soluble cyclophanes for host-guest chemistry. Introducing various functional side chains on the amino groups of DPM permits the cyclophanes to exhibit controlled guest-binding and supramolecular aggregation behavior[6] by stimuli-responsiveness such as redox,[6,7] pH,[7,8] and temperature.[8,9] On the other hand, several DPM-based chemical sensors have been reported. Bi's and Zhao's groups prepared zinc(II) ion sensors by forming a Schiff base on the amino groups.[10,11] Goswami's group showed that the aniline units could be converted to a Schiff base to detect zinc(II) ion and HSO_4^-, accompanying changes in fluorescence spectra.[12] In these cases, the compounds have the same structures around the amino groups, and the structural feature of DPM

comprising two aniline units is not fully utilized. Therefore, we demonstrated that DPM could be applied as a platform for proton, pH, and metal ion sensors derived from the electronic and synthetic advantages of DPM by assigning different roles to the two amino groups of DPM.

From the viewpoint of the structural features of DPM, one of the aniline units acts as an electron donor, and the amino group is a Brønsted base acting as a proton acceptor. Moreover, the amino group can be converted to a Schiff base as a metal ion ligand by reacting with 2-formylpyridine. Additionally, an imide is suitable for introducing a fluorescent acceptor into a DPM-based fluorescent probe. Among imides, diarylmaleimide is an excellent fluorophore strongly influencing the substituted aryl groups,[13–19] and maleimide skeletons are promising fluorophores for external stimuli-responsive involving photoinduced electron transfer (PeT).[20,21] Based on the above points, we designed **1**, in which 4-methoxyphenyl groups as the aryl groups of diarylmaleimide showing charge-transfer-type fluorescence[13] are adapted (Figure 1). **1** is expected to exhibit a turn-off/on fluorescence property by the protonation or the metalation, accompanying the conversion to a Schiff base, of the amino group. Herein, we demonstrated the proton, pH, and metal ion stimuli-responsive fluorescent probe based on DPM and showed that DPM is available as a platform for sensing molecules.

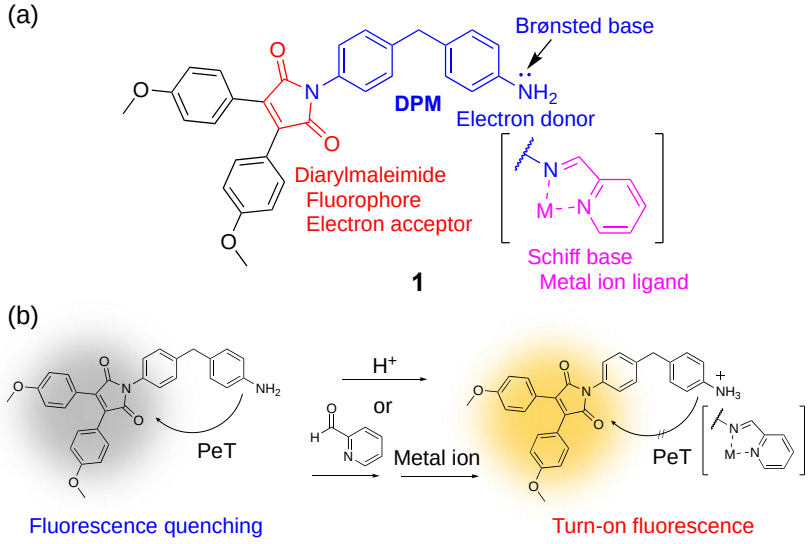

Figure 1. (a) The design of the fluorescent probe based on DPM **1**. (b) The turn-on fluorescence by protonation or formation of the Schiff base and its metalation.

RESULTS AND DISCUSSION

The synthetic routes of **1** are shown in Scheme 1. The synthesis started with protecting one amino group in DPM by *tert*-butoxycarbonyl (Boc) to give **2**. Imidization of the other amino group in **2** was achieved by reacting to 2,3-dichloromaleic anhydride to form **3**. The introduction of the aryl groups to the imide unit was carried out by Suzuki coupling to yield **4**, followed by deprotecting the Boc group by trifluoroacetic acid (TFA) to give **1**.

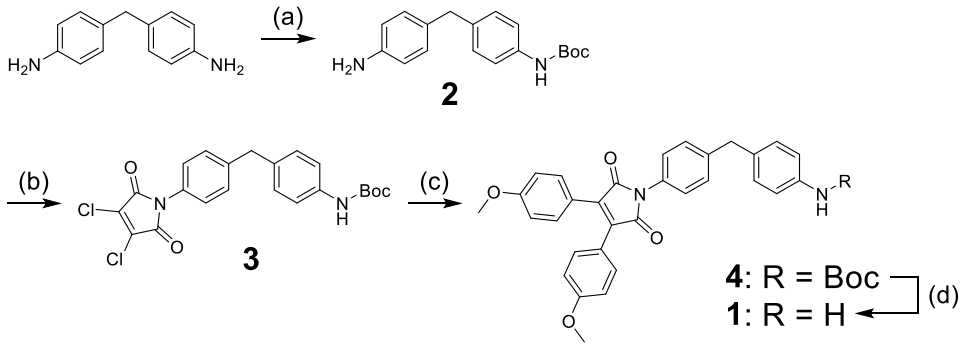

Scheme 1. Synthesis of **1**. (a) Boc_2O, Et_3N, CH_2Cl_2, rt, 3 h, 49%. (b) 2,3-dichloromaleic anhydride, toluene, reflux, 1 day, 89%. (c) 4-methoxyphenylboronic acid, $Pd(OAc)_2$, XPhos, K_3PO_4, toluene, 100 ºC, 1 day, 84%. (d) TFA, CH_2Cl_2, rt, 2 h, 94%.

The absorption spectral peaks of **1** are summarized in Table 1. The absorption peak in the longest wavelength of **1** in MeCN was observed at 402 nm (Figure S1), and this band is derived from the diarylmaleimide unit. After adding an excess TFA to the solution, the absorption band in the longest wavelength did not show a significant change, suggesting that TFA has little effect on the diarylmaleimide unit. The spectral absorption changes of **1** in CH_2Cl_2 and toluene were similar to those in MeCN.

Table 1. Summary of the absorption spectral peaks of **1** in MeCN, CH_2Cl_2, and toluene before and after adding an excess amount of TFA.

	λ_{max} / nm (ε / 10^3 M^{-1} cm^{-1})		
	MeCN	CH_2Cl_2	toluene
1	402 (5.78), 315 (8.66), 243 (32.5)	412 (6.60), 332 (9.76), 245 (33.5)	415 (5.96), 328 (9.86)
1+TFA	402 (6.03), 324 (8.68), 239 (30.4)	413 (6.49), 332 (9.19), 243 (29.1)	414 (6.30), 328 (9.68)

Titration of TFA into **1** in MeCN, CH_2Cl_2, and toluene was carried out to evaluate the proton stimuli-responsive fluorescent behavior of **1**, and the results are shown in Figure 2. **1** in MeCN exhibited a weak fluorescence band at 546 nm, and the increase of the fluorescence intensity was observed upon the gradual addition of TFA and a red-shift of λ_{max} to 557 nm (Figure 2a). The fluorescence intensity of **1** in CH_2Cl_2 also increased by responsiveness to TFA, and the fluorescence band was slightly shifted from 554 nm to 557 nm (Figure 2b). Similarly, the fluorescence spectral change of **1** in toluene was observed upon the

addition of TFA with a slight shift of λ_{max} from 550 nm to 551 nm (Figure 2c). The fluorescence bands of **1** appearing upon the addition of TFA in three solutions agreed with the fluorescence band of *N*-methyl-bis(4-methoxyphenyl)maleimide in CH_2Cl_2, exhibiting at 551 nm.[13] The fluorescence of **1**, therefore, originated from the bis(4-methoxyphenyl)maleimide unit in **1**.

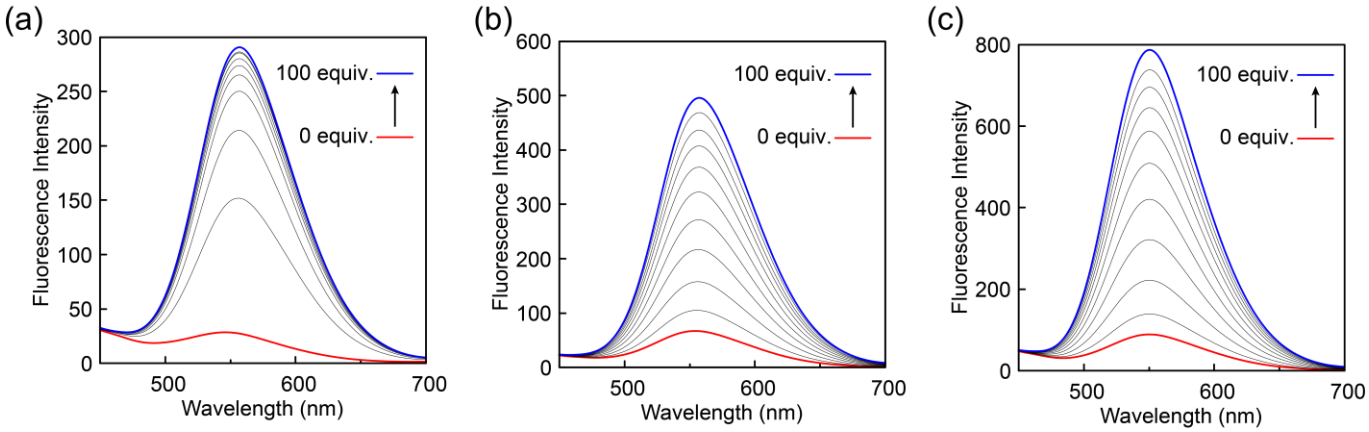

Figure 2. Fluorescence spectral change of **1** (50 μM) upon the gradual addition of TFA in (a) MeCN, (b) CH_2Cl_2, and (c) toluene (λ_{ex} = 400 nm).

The reversible change of the fluorescent behavior of **1** in MeCN and MeOH (1:1 v/v) was investigated by adding TFA and DBU alternately (Figure S2). The fluorescence band originating from **1** protonated by TFA disappeared upon adding DBU, and the further addition of TFA recovered the fluorescence intensity, although the responsiveness for TFA became poor.

The NMR spectral change of **1** upon adding TFA was observed in $CDCl_3$ (Figure S3). The aromatic protons (H_a and H_b) of the aniline unit in **1** appeared at 6.65 and 7.00 ppm, respectively, and these signals were dramatically shifted to approximately 7.26 ppm upon the addition of TFA. The signal of the methylene protons (H_c) also showed a low magnetic field shift from 3.91 ppm to 4.05 ppm. As expected, the results indicated that the amino group is converted to the ammonium cation upon the addition of TFA.

Based on the results of the fluorescence and NMR measurements, the turn-on fluorescence behavior observed for the proton sensor **1** is due to the protonation of the aniline unit and the subsequent halt of the PeT from the amino group to the excited maleimide fluorophore.

To further develop the applications, the fluorescent behavior of **1** in a mixture of MeCN and various pH buffers was investigated. **1** in a mixture of MeCN and pH 3.1 of citrate buffer (5:5 v/v) exhibited a fluorescence peak at 575 nm, red-shifted from that in only MeCN (557 nm), and the fluorescence peak of **1** was red-shifted with increasing citrate buffer ratio (580 nm, 4:6 v/v; 587 nm, 3:7 v/v; 594 nm, 2:8 v/v) (Figure 3a), reflecting that the charge-transfer-type fluorescence property of **1** was affected by the polarity increase. The spectral change for buffer pH (50 mM, citrate buffer: pH 3.1, 4.1, 5.0, 5.8; 100 mM, phosphate

buffer: pH 7.3) was examined in the 4:6 v/v ratio (Figure 3b). Notably, the fluorescence intensity originating from **1** increased with decreasing the pH value of the buffer from 5.0 to 3.1. When the buffer pH 3.1 and 4.1 were used, the fluorescence properties were enhanced, reflecting the protonation of the amino group. A slight enhancement of the fluorescence of **1** was observed in the mixture of MeCN and the buffer pH 5.0. On the other hand, no fluorescent responsiveness of **1** was observed in the mixture of MeCN and the pH 5.8 and 7.3 of buffers. The pK_a of the amino group is evaluated to be 3.1-4.1, which is consistent with that of aniline (pK_a 3.82 in DMSO),[22] based on the significant fluorescence spectral change between the buffer pH 4.1 and 3.1.

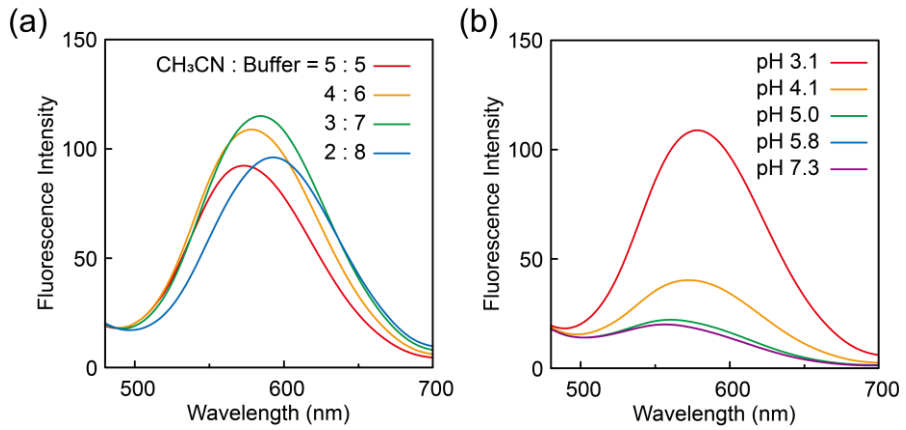

Figure 3. (a) Fluorescence spectra of **1** (50 μM) in various ratios of MeCN to citrate buffer (50 mM, pH 3.1) (MeCN / buffer = 5:5, 4:6, 3:7, 2:8 v/v) (λ_{ex} = 400 nm). (b) Fluorescence spectra of **1** (50 μM) in the mixture of MeCN and citrate buffer (50 mM, pH 3.1, 4.1, 5.0, 5.8) or phosphate buffer (100 mM, pH 7.3) (λ_{ex} = 400 nm, MeCN / buffer = 4:6 v/v).

The demonstrations that **1** works as a proton and pH-sensitive probe were performed. The subsequent study examined **1** as a metal ion sensor by forming a Schiff base. 2-Formylpyridine (**pyCHO**) was adopted as an aldehyde for a Schiff base formation with **1**, while zinc(II), nickel(II), and copper(II) ions were chosen in a proof-of-principle experiment. The syntheses of the Schiff base **1py** and the metalized zinc ion **1pyZn** were attempted (Scheme 2), but both compounds could not be isolated, although the formation of these compounds was confirmed by ^{1}H NMR and MALDI-TOF MS (Figures S4-S6). Moreover, ^{1}H NMR spectra indicated the existence of an equilibrium between **1pyZn**, **1py**, and **1**, because the Schiff base formation is reversible. To examine the property of **1** as a metal ion sensor, **1py** and **1pyZn** were formed in the measurement system without isolation. A solution of **1** (50 μM), **pyCHO** (100 equiv.), and $Zn(OAc)_2$•$2H_2O$ (10 equiv.) in MeCN and MeOH (1:1 v/v) was prepared, and its fluorescence property was measured (Figure 4a). The fluorescence intensity was increased with time, and MALDI-TOF MS of the resulting solution showed the formation of **1pyZn** (Figure S7a). On the other hand, the absence of $Zn(OAc)_2$•$2H_2O$

led to a slight increase in the intensity (Figure 4b), and when **pyCHO** was not added, the fluorescence spectrum did not change (Figure 4c). From the ^{1}H NMR spectra results of **1py**, the signals derived from the aromatic protons in the aniline unit (H_e and H_d) shifted to a low magnetic field region compared with those of **1** (H_a and H_b) (Figure S5), suggesting that the formation of **1py** reduces the donation ability of the aniline unit and improves its fluorescence intensity. However, **1py** is in the equilibrium state between **1**, and the formation of **1py** is not enough in this measuring system from the fluorescence spectra. In the presence of zinc(II) ion, **1py** is metalized with time. The metalation, forming **1pyZn**, fixes and promotes the Schiff base structure, enhancing the fluorescence intensity. That is, zinc(II) ion can be detected by the combination of **1** and **pyCHO**, which turns on the fluorescence. Another possibility is that zinc(II) ion coordinates the carbonyl group of **pyCHO** to activate the reactivity and promote the imine formation, and then the chelation occurs. A mixture of $Zn(OAc)_2$•$2H_2O$ and **pyCHO** without **1** did not show a significant fluorescence band around 550 nm, suggesting that the excess **pyCHO** and metal ions do not affect the fluorescence behavior of the **1pyZn** system (Figure S8). Nickel(II) ion was also attempted, and the turn-on behavior was observed, like the zinc(II) ion sensing system (Figure 5). The MALDI-TOF MS measurements showed the formation of **1pyNi** (Figure S7b), indicating that nickel(II) ion was also metalized to **1py**, enhancing the fluorescence intensity. Consequently, the Schiff base formation between **1** and **pyCHO** was found to be accelerated by zinc and nickel ions suitable for the chelate metal complexes. On the other hand, when $Cu(OAc)_2$•H_2O was used, the enhancement of the fluorescence intensity was observed with and without **pyCHO** (Figure 5c, d). The copper(II) ion coordinates with a lone pair on the amino group, and the PeT is halted.[21]

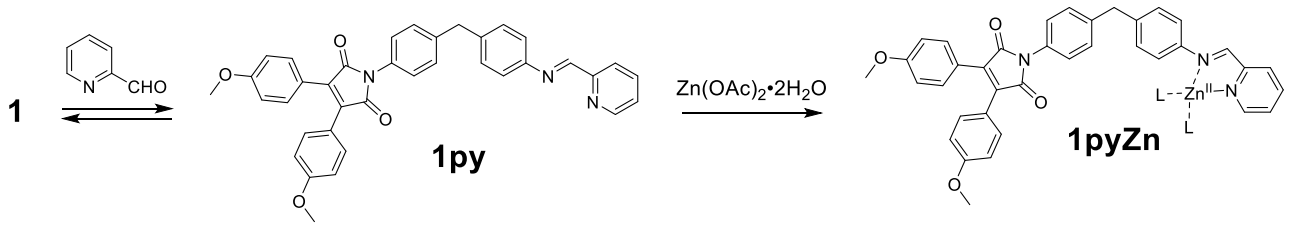

Scheme 2. Formation of **1py** and **1pyZn**

Lin's group has reported that *N*-arylmaleimide, including dimethylamine, detects metal ions selectively, and applying the selectivity permits the construction of logic gates.[21] Similar to the report, the metal sensing system of **1** was applied to an AND circuit. In the proposed AND circuit system, **pyCHO**, metal (nickel or zinc) ion, and time as inputs are used in the presence of **1**, and a more than three-fold enhancement of fluorescence intensity ($I/I_0 > 3$) is adapted as an output (Figure 6). The output signal is obtained by the following procedure: **1**, **pyCHO**, and nickel(II) (or zinc(II)) ion are mixed, and the solution is held for 1 h. In the other cases, the output is not turned on since the fluorescence intensity is enhanced less than three-

fold. In such a manner, **1** with combining **pyCHO** is available to the AND circuit as well as the metal sensing.

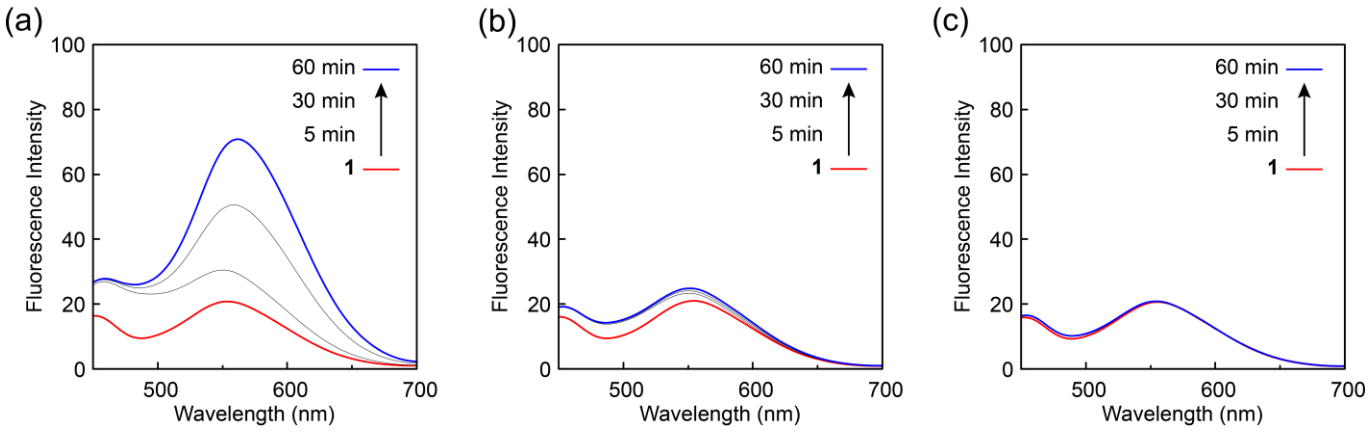

Figure 4. Fluorescence spectral change of **1** (50 μM) in MeCN and MeOH (1:1 v/v) upon the addition of (a) 2-formylpyridine (100 equiv.) and $Zn(OAc)_2$•$2H_2O$ (10 equiv.), (b) 2-formylpyridine (100 equiv.), and (c) $Zn(OAc)_2$•$2H_2O$ (10 equiv.) (λ_{ex} = 400 nm).

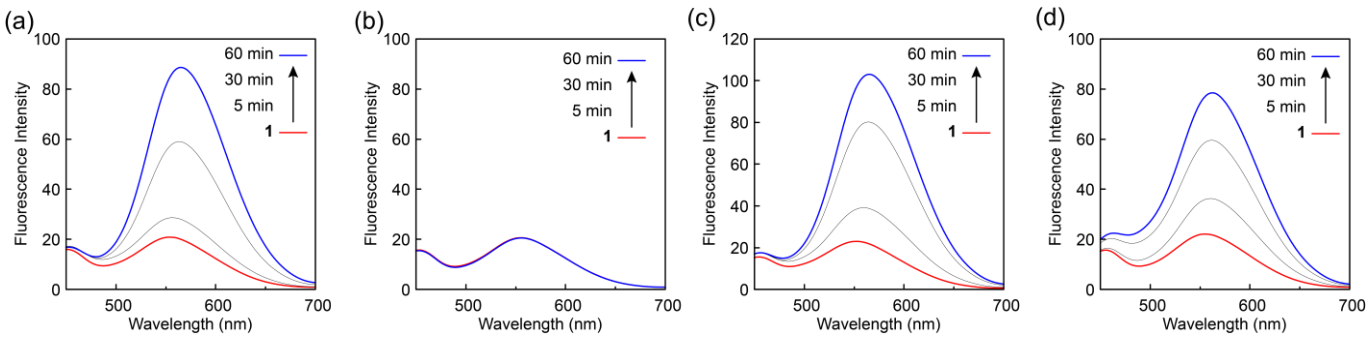

Figure 5. Fluorescence spectral change of **1** (50 μM) in MeCN and MeOH (1:1 v/v) upon the addition of (a) 2-formylpyridine (100 equiv.) and $Ni(OAc)_2$•$4H_2O$ (10 equiv.), (b) $Ni(OAc)_2$•$4H_2O$ (10 equiv.), (c) 2-formylpyridine (100 equiv.) and $Cu(OAc)_2$•H_2O (10 equiv.), and (b) $Cu(OAc)_2$•H_2O (10 equiv.) (λ_{ex} = 400 nm).

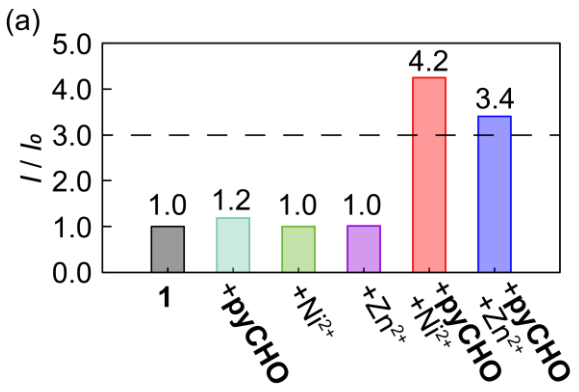

(b)

input				output
1	**pyCHO**	Ni^{2+} (Zn^{2+})	1 h	$I / I_0 > 3$
1	0	0	0	0
1	1	0	0	0
1	0	1	0	0
1	0	0	1	0
1	1	1	0	0
1	1	0	1	0
1	1	1	1	1

Figure 6. (a) The ratio for **1** of fluorescence spectral change after 1 h preparing the solution. (b) The truth table of the AND circuit.

In summary, a new DPM-based fluorescent probe **1**, including diarylmaleimide as a fluorophore, was designed to utilize the synthetic and electronic advantages of DPM fully, and the fluorescence properties were examined to show that DPM can be used as a platform for proton, pH, and metal ion sensors. **1** in MeCN, CH_2Cl_2, and toluene exhibited the responsiveness for TFA. Measuring the ^{1}H NMR spectra of **1** in $CDCl_3$ confirmed that the amino group of the aniline unit was protonated by TFA, as expected. The fluorescence spectral change of **1** in a mixture of MeCN and various pH buffers was investigated, and it was revealed that the fluorescence property of **1** was affected by the pH buffers. Moreover, the combination of **1** and **pyCHO** detected metal (zinc or nickel) ion by enhancing the fluorescence, reflecting the formation of the Schiff base skeleton and its metalation. Additionally, this system was applied to an AND circuit. According to the above results, we succeeded in demonstrating that the DPM-based molecule **1**, including diarylmaleimide, could detect proton, pH, and metal ions; that is, the DPM skeleton is available as a platform for fluorescent probes.

EXPERIMENTAL

Synthesis of 2. A mixture of 4,4'-diaminodiphenylmethane (1.98 g, 10.0 mmol), NEt_3 (1.39 mL, 10.0 mmol), di-*tert*-butyl dicarbonate (2.17 g, 9.94 mmol), and CH_2Cl_2 (100 mL) was stirred in room temperature for 3 h. The reaction mixture was concentrated under reduced pressure, and the residue was purified by silica gel column chromatography (EtOAc/Hexane = 1:2) to give **2** (1.47 g, 49%) as a white powder. ^{1}H NMR (400 MHz, $CDCl_3$): δ 1.50 (s, 9H), 3.81 (s, 2H), 6.38 (br, 1H), 6.61 (d, J = 8.2 Hz, 2H), 6.95 (d, J = 8.1 Hz, 2H), 7.08 (d, J = 8.5 Hz, 2H), 7.23 (d, 2H); ^{13}C NMR (100 MHz, $CDCl_3$): δ 28.4, 40.4, 80.4, 115.3, 118.8, 129.3, 129.7, 131.4, 136.2, 136.6, 144.4, 152.9.

Synthesis of 3. A mixture of **2** (1.34 g, 4.50 mmol), 2,3-dichloromaleic anhydride (0.908 g, 5.45 mmol), and toluene (120 mL) was refluxed for 1 day. After cooling to room temperature, the reaction mixture was directly charged in silica gel chromatography and purified (EtOAc/Hexane = 1:3) to give **3** (1.79 g, 89%) as a pale-yellow powder. ^{1}H NMR (400 MHz, $CDCl_3$): δ 1.51 (s, 9H), 3.96 (s, 2H), 6.42 (br, 1H), 7.11 (d, J = 8.5 Hz, 2H), 7.22-7.30 (m, 6H); ^{13}C NMR (100 MHz, $CDCl_3$): δ 28.3, 40.8, 80.5, 118.9, 126.0, 128.5, 129.6, 129.7, 133.6, 134.8, 136.7, 142.2, 152.8, 162.0; MS (MALDI-TOF) *m/z*: $[M+Na]^+$ calcd for $C_{22}H_{20}Cl_2N_2O_4Na$ 469.07; Found 469.59. Anal. Calcd for $C_{22}H_{20}Cl_2N_2O_4$: C, 59.07; H, 4.51; N, 6.26. Found: C, 59.06; H, 4.64; N, 6.06.

Synthesis of 4. A mixture of **3** (90.0 mg, 0.20 mmol), 4-methoxyphenylboronic acid (73.8 mg, 0.48 mmol), palladium acetate (4.8 mg, 0.021 mmol), XPhos (19.6 mg, 0.041 mmol), tripotassium phosphate (84.8 mg, 0.40 mmol), and toluene (3.0 mL) was heated at 100 °C in a nitrogen atmosphere for 1 day. After cooling to room temperature, the reaction mixture was directly charged in silica gel chromatography and purified

(EtOAc/Hexane = 1:3) to give **4** (99.5 mg, 84%) as a yellow powder. ^{1}H NMR (400 MHz, $CDCl_3$): δ 1.51 (s, 9H), 3.84 (s, 6H), 3.97 (s, 2H), 6.41 (br, 1H), 6.89 (m, 4H), 7.13 (d, J = 8.5 Hz, 2H), 7.25-7.30 (m, 4H), 7.34 (m, 2H), 7.52 (m, 4H); ^{13}C NMR (100 MHz, $CDCl_3$): δ 28.4, 40.9, 55.3, 80.4, 114.2, 118.8, 121.2, 126.2, 129.4, 129.6, 129.9, 131.6, 134.2, 135.2, 136.6, 140.8, 152.8, 160.8, 170.1; MS (MALDI-TOF) *m/z*: $[M+Na]^+$ calcd for $C_{36}H_{34}N_2O_6Na$ 613.23; Found 613.50. Anal. Calcd for $C_{36}H_{34}N_2O_6$: C, 73.20; H, 5.80; N, 4.74. Found: C, 73.19; H, 6.00; N, 4.66.

Synthesis of 1. A mixture of **4** (70.5 mg, 0.119 mmol), trifluoroacetic acid (1.0 mL), and CH_2Cl_2 (20 mL) was stirred at room temperature for 2 h. The reaction mixture was washed with saturated $NaHCO_3$ aq. The organic layer was dried with $MgSO_4$ and filtered. The filtrate was concentrated under reduced pressure. The residue was purified by silica gel column chromatography (EtOAc/Hexane = 1:1) to give **1** (55.3 mg, 94%) as an orange powder. Further purification was carried out by recrystallization from EtOAc and hexane. ^{1}H NMR (400 MHz, $CDCl_3$): δ = 3.84 (s, 6H), 3.91 (s, 2H), 6.65 (m, 2H), 6.90 (m, 4H), 7.00 (d, J = 8.4 Hz, 2H), 7.28 (d, 2H), 7.33 (m, 2H), 7.52 (m, 4H); ^{13}C NMR (100 MHz, $CDCl_3$): δ 40.7, 55.3, 114.1, 115.5, 121.2, 126.1, 129.4, 129.7, 129.9, 130.8, 131.6, 134.2, 141.5, 144.4, 160.8, 170.2; MS (MALDI-TOF) *m/z*: $[M+H]^+$ calcd for $C_{31}H_{27}N_2O_4$ 491.20; Found 491.79. Anal. Calcd for $C_{31}H_{26}N_2O_4 \bullet 0.25H_2O$: C, 75.21; H, 5.40; N, 5.66. Found: C, 75.17; H, 5.41; N, 5.47.

Protonation of 1 by TFA for ^{1}H NMR spectra.

To a solution of **1** in $CDCl_3$, one drop of TFA (excess) was added, and the ^{1}H NMR measurement was carried out.

Preparation of 1py for ^{1}H NMR spectra. To a solution of **1** in MeCN (4.0 mM, 1.0 mL), a solution of 2-formylpyridine in MeCN (12.5 mM, 0.32 mL) and MeOH (0.32 mL) was added. The mixture was stirred at room temperature for 1 day. The reaction mixture was dried, and the residue was dissolved in $CDCl_3$ to prepare the sample for ^{1}H NMR measurement. After keeping for 1 day, the ^{1}H NMR measurement was carried out.

Preparation of 1pyZn for ^{1}H NMR spectra. To a solution of **1** in MeCN (4.0 mM, 1.0 mL), solutions of 2-formylpyridine in MeCN (12.5 mM, 0.32 mL) and $Zn(OAc)_2 \bullet 2H_2O$ in MeOH (12.5 mM, 0.32 mL) were added. The mixture was stirred at room temperature for 1 day. The reaction mixture was dried, and the residue was dissolved in $CDCl_3$ to prepare the sample for ^{1}H NMR measurement. After keeping for 1 day, the ^{1}H NMR measurement was carried out.

Preparation of the solution for metal sensing. To the solution of **1** in a mixture of MeCN and MeOH (1:1 v/v) (50 μM, 3.0 mL), solutions of 2-formylpyridine in MeOH (1.5 M, 10 μL) and $Zn(OAc)_2 \bullet 2H_2O$ or $Ni(OAc)_2 \bullet 4H_2O$ in MeOH (0.15 M, 10 μL) or $Cu(OAc)_2 \bullet H_2O$ in MeOH (0.015 M, 100 μL) were added.

ACKNOWLEDGEMENTS

This work was supported by JSPS KAKENHI Grant Numbers 20K15262.

REFERENCES

1. Z. Sun, M. Liu, L. Yi, and Y. Wang, *RSC Adv.*, 2013, **3**, 7271.
2. H.-K. Luo, C. Wang, W. Rusli, C.-Z. Li, E. Widjaja, P.-K. Wong, L. P. Stubbs, and M. Van Meurs, *J. Organomet. Chem.*, 2015, **798**, 354.
3. X. Zhi, H. Bi, Y. Gao, J. Liu, J. Chen, K. Gao, and X. Zhang, *Chem. Lett.*, 2019, **48**, 654.
4. B. Wei, W. Li, Z. Zhao, A. Qin, R. Hu, and B. Z. Tang, *J. Am. Chem. Soc.*, 2017, **139**, 5075.
5. S. Bandi and D. K. Chand, *Chem. Eur. J.*, 2016, **22**, 10330.
6. O. Hayashida and K. Shibata, *J. Org. Chem.*, 2020, **85**, 5493.
7. O. Hayashida, Y. Tanaka, and T. Miyazaki, *Molecules*, 2021, **26**, 3097.
8. O. Hayashida, T. Tomita, and T. Miyazaki, *Chem. Lett.*, 2021, **50**, 1611.
9. O. Hayashida and H. Tanaka, *Chem. Lett.*, 2020, **49**, 605.
10. S. Liu, C. Bi, Y. Fan, Y. Zhao, P. Zhang, Q. Luo, and D. Zhang, *Inorg. Chem. Commun.*, 2011, **14**, 1297.
11. W. Wang, R. Li, T. Song, C. Zhang, and Y. Zhao, *Spectrochim. Acta A. Mol. Biomol. Spectrosc.*, 2016, **164**, 133.
12. S. Goswami, S. Das, K. Aich, D. Sarkar, and T. K. Mondal, *Tetrahedron Lett.*, 2013, **54**, 6892.
13. H.-C. Yeh, W.-C. Wu, and C.-T. Chen, *Chem. Commun.*, 2003, 404.
14. H. Xie, L. Ho, M. Truelove, B. Corry, and S. Stewart, *J. Fluoresc.*, 2010, **20**, 1077.
15. K. Onimura, M. Matsushima, M. Nakamura, T. Tominaga, K. Yamabuki, and T. Oishi, *J. Polym. Sci. Part Polym. Chem.*, 2011, **49**, 3550.
16. M. H. Lauer, R. L. Drekener, C. R. D. Correia, and M. H. Gehlen, *Photochem. Photobiol. Sci.*, 2014, **13**, 859.
17. J. Wang, R. Zheng, H. Chen, H. Yao, L. Yan, J. Wei, Z. Lin, and Q. Ling, *Org. Biomol. Chem.*, 2018, **16**, 130.
18. J. Wang, Z. Liu, S. Yang, Y. Lin, Z. Lin, and Q. Ling, *Chem. Eur. J.*, 2018, **24**, 322.
19. J. Price, E. Albright, A. Decken, and S. Eisler, *Org. Biomol. Chem.*, 2019, **17**, 9562.
20. Q. Huang, Z. Liu, L. Huang, Z. Lin, and Q. Ling, *J. Mater. Chem. C*, 2019, **7**, 13904.
21. X. Zheng, Z. Liu, D. Xiao, J. Sun, Z. Lin, and Q. Ling, *J. Photochem. Photobiol. Chem.*, 2020, **401**, 112775.
22. M. R. Crampton and I. A. Robotham, *J. Chem. Res. (S)*, 1997, 22.